Polymer 50 (2009) 1516–1525

Contents lists available at ScienceDirect

Polymer

journal homepage: www.elsevier.com/locate/polymer

Self-association and microenvironment of random amphiphilic copolymers of sodium *N*-acryloyl-L-valinate and *N*-dodecylacrylamide in aqueous solution

Pranabesh Dutta [a], Joykrishna Dey [a,*], Goutam Ghosh [b], Rati Ranjan Nayak [c]

[a] Department of Chemistry, Indian Institute of Technology, Kharagpur 721302, India
[b] UGC-DAE Consortium for Scientific Research, BARC, Trombay, Mumbai 400 085, India
[c] Department of Polymer Chemistry, Kyoto University, Katsura, Nishikyo-ku, Kyoto 615 8510, Japan

ARTICLE INFO

Article history:
Received 5 August 2008
Received in revised form
19 December 2008
Accepted 25 December 2008
Available online 20 January 2009

Keywords:
Polymer
Fluorescence
Transmission electron microscopy

ABSTRACT

The present paper reports on the syntheses and association behavior of two random copolymers of sodium *N*-acryloyl-L-valinate and *N*-dodecylacrylamide in buffered (pH 8.0) aqueous solution containing 0.1 M NaCl. Surface tension and viscosity results showed pronounced amphiphilic nature of the copolymers in aqueous solution at pH 8.0. Steady-state fluorescence studies using pyrene and *N*-phenyl-1-naphthylamine as probe molecules suggested microdomain formation through interpolymer association above a critical concentration called 'critical aggregation concentration' (CAC) as low as ca. 10^{-3} g L^{-1}. The local polarity of the hydrophobic domain formed in aqueous solution was estimated from steady-state fluorescence spectra of pyrene. The microviscosity of the domains was evaluated using 1,6-diphenyl-1,3,5-hexatriene as a fluorescent probe using steady-sate fluorescence depolarization and time-resolved fluorescence method. Dynamic light scattering technique was performed over a wide range of concentration to determine hydrodynamic size of the aggregates. It was observed that both copolymers retain rather open conformation in dilute solutions having polymer concentrations less than CAC. However, with increase in concentration the intermolecular association becomes favorable towards the formation of more compact aggregates. The transmission electron microscopic images of both copolymers at a concentration above CAC revealed spherical aggregates of uniform diameter (~50 nm).

1. Introduction

Current research has drawn interest for synthetic polymers including polypeptides, and related poly(amino acids) owing to their biocompatibility, biodegradability and various biological activities [1]. They form a variety of aggregated structures in solution through the intra- and intermolecular interactions [2,3]. The self-association is driven by the hydrogen-bonding, electrostatic, and hydrophobic interactions. Since these synthetic polymers serve as model systems for biopolymers, a thorough investigation of the mechanism and the factors influencing these interactions is important. To mimic biopolymers, poly(*N*-acryloyl-L-amino acid) has emerged as a promising biomaterial. Consequently, a variety of poly(acrylamide)s and poly(methacrylamide)s of different amino acids have been synthesized to study their characteristic polymerization behavior, structures, and properties [4]. Because of their unique properties, these polymers are not only of fundamental interest but also have many potential applications, such as optically active adsorbents [5], photochromic materials [6], chiral recognition stationary phases, and metal ion absorbents [7]. These can serve even as a vehicle for chiral purification media and controlled release system [8,9]. Casolaro et al. have studied the conformational behavior of poly(*N*-acryloyl-L-amino acid) with L-valine and L-leucine residues in view of their application in chemical valve system [10,11]. These homopolymers are typical polyelectrolyte in nature. They contain isopropyl and amido groups which provide improved temperature sensitivity as in the case of uncharged p(NIPAAm). Also the ionizable carboxyl groups make them responsive to pH [12,13]. Domb et al. [14] have reported that poly(*N*-acryloyl amino acid)s bearing tyrosine, leucine, phenylalanine, *tert*-leucine, and proline residues are active as heparanase inhibitors and release of basic fibroblast growth factor from the extracellular matrix, whereas *trans*-hydroxyproline, glycine, and serine containing polymers were active only as heparanase inhibitors. It was found that a net anionic charge (i.e. carboxylate group) is essential for biological activity of these systems.

More recently, hydrophobically modified amino acid-based water-soluble polymers have become a subject of interest [15,16].

* Corresponding author. Tel.: +91 3222 283308; fax: +91 3222 255303.
E-mail address: joydey@chem.iitkgp.ernet.in (J. Dey).

0032-3861/$ – see front matter © 2009 Elsevier Ltd. All rights reserved.
doi:10.1016/j.polymer.2008.12.049

This is because these amphiphilic polymers undergo intra- or interpolymeric hydrophobic associations or at the same time both types of associations to form micelle-like clusters, which may find applications in different fields [17], such as personal care formulations, protein solubilization, and drug delivery. Continuing emergence of advanced applications motivated us to study the aggregation behavior of hydrophobically modified poly(*N*-acryloyl-L-amino acid), which is supposed to be promising biomaterial. It is anticipated that hydrophobically modified poly(*N*-acryloyl-L-amino acid) will self-assemble to form secondary structures with a better compatibility with biological system and interact favorably with protein, enzymes, or lipids. This prospective property may result in hydrophobically modified amino acid-based chiral polyelctrolyte with some innovative applications. With this in mind, we have synthesized random copolymers of sodium *N*-acryloyl-L-valinate (SAVal) and *N*-dodecylacrylamide (DA) with different copolymer compositions (see Fig. 1). In a preliminary report [15], we have demonstrated hydrophobic domain formation by these copolymers in dilute aqueous solutions. Sato and coworkers [16] have also reported the aggregation behavior of similar copolymers having different hydrophobe contents. These authors have shown that the amphiphilic copolymers form flower-like unimer micelles and multipolymer unicore micelles, with the hydrophobic core protected by the hydrophilic loops in aqueous solution through intra- and interpolymer interactions, respectively. They have concluded that the copolymer with hydrophobe content less than 10% forms multipolymer unicore micelles through interpolymer hydrophobic association. On the other hand, the copolymer with hydrophobe content greater than 10% forms both unimer micelles and multipolymer unicore micelles. The molecular weights of these polymers, however, were relatively lower with shorter chain lengths. It is quite obvious that association behavior of such polymers should also be a strong function of chain length. Therefore, we have undertaken the present study to shed some light on the self-assembly and conformational behavior of this novel class of amphiphilic chiral copolymers in aqueous media. We focus here on the influence of polymer structural parameter like polymer molecular weight. Aiming at investigating how chain length affects the formation and size and microenvironment of micelle-like clusters of polymer chains, we report in this paper the synthesis and characterization of this new class of amphiphilic polymers using surface tension, viscometry, fluorescence, dynamic light scattering, and microscopic techniques.

2. Experimental section

2.1. Materials

Dodecylamine (SRL), L-valine, acryloyl chloride, (Aldrich), $CDCl_3$, D_2O, and CD_3OD (Aldrich) were used without further purification. 2,2′-azobis(isobutyronitrile) (AIBN) was recrystallized from methanol. The fluorescence probes like pyrene, 1,6-diphenyl-1,3,5-hexatriene (DPH), and *N*-phenyl-1-naphthylamine (NPN) (Aldrich) were recrystallized from ethanol or acetone–ethanol mixture at least three times before use. Purity of all the probes was tested by the fluorescence emission and excitation spectra. All the reagents and solvents specially dimethylformamide (DMF), ethanol, methanol, tetrahydrofuran (THF), acetone, dichloromethane were of good quality commercially available and were dried and distilled fresh before use. Analytical grade sodium chloride, potassium chloride, sodium dihydrogen phosphate, and sodium hydroxide were procured from SRL, Mumbai. Double distilled water was used for preparation of all solutions.

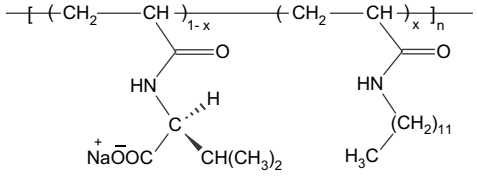

Fig. 1. Chemical structure of the copolymers.

2.2. Synthesis of monomers

N-Acryloyl-L-valine (AVal) was prepared by the procedure similar to one previously reported [16,18]. Briefly, to a well-stirred aqueous solution of L-valine (3.1 g, 0.02 mol) and sodium bicarbonate (1.6 g, 0.04 mol) in twice distilled water (20 mL) was added dropwise acryloyl chloride (1.79 g, 0.020 mol) over a 30 min period. The temperature of the reaction mixture was maintained at about 5–10 °C throughout addition. The reaction mixture was stirred at room temperature for additional 2 h. Finally the pH of the reaction mixture was dropped down to 2 with 1 M HCl. Aqueous solution was then extracted with ethylacetate. The organic phase was dried over magnesium sulphate and the solvent was evaporated in vacuo at 30 °C. The white powder thus obtained was recrystallized in ethylacetate/ether (1:1 v/v) mixture. The compound was characterized by ^{1}H NMR and FT-IR spectroscopies. Yield 70%; M.P 110–112 °C; $[\alpha]_D^{25}$ (1%, CH_3OH) = −13.34° FT-IR (KBr, cm^{-1}): 3341 (N–H stretching); 2972 and 2940 (C–H stretching); 1734 (COOH); 1651 (amide-I band); 1611 (–C═C– stretching); 1546 (amide-II band); 1468, 1418, 1326, 1216, 1162, 1070, 993, 968, 934, 811, 741, 636. ^{1}H NMR (200 MHz, $CDCl_3$): δ (δ in ppm, J in Hz): 7.46 (br s, 1H, N*H*), 6.45 (dd, 1H, $J_{trans} = 17.5$, $J_{cis} = 8.108$, H_2C═C*H*), 6.20 (dd, 1H, $J_{gem} = 1.502$, $J_{trans} = 17.5$, H*H*C═CH–), 5.73 (dd, 1H, $J_{gem} = 1.502$, $J_{cis} = 8.108$, *H*HC═CH–), 4.65 (t, 1H, $J = 5.82$, NH–C*H*–COOH), 2.25 (m, 1H, C*H*(CH_3)$_2$), 0.97 (d, 6H, CH(*CH*$_3$)$_2$).

Sodium *N*-acryloyl-L-valinate (SAVal) was prepared by stirring with equimolar amounts of sodium bicarbonate in water–THF mixture (1:1 v/v) for 24 h. The product obtained as solid mass after solvent evaporation and freeze-drying was purified from ethanol–acetone mixture (1:5 v/v) to remove the unreacted acid.

N-Dodecylacrylamide (DA) was prepared by acylation of the dodecylamine with acryloyl chloride in THF using triethylamine as base according to the method reported by Morishima et al. [19]. The compound was recrystallized in ethanol/water mixture. Finally the compound was chemically identified by ^{1}H NMR and FT-IR spectroscopies. Yield 86%; M.P 53–55 °C; FT-IR (KBr, cm^{-1}): 3271 cm^{-1} (N–H stretch); (1652 cm^{-1}) C═O stretch, amide-I; (1551 cm^{-1}) N–H bend, amide-II; 1620 (–C═C– stretching), 1474, 1407, 1243, 993, 964, 809, 721, 698; ^{1}H NMR (200 MHz, $CDCl_3$), δ (δ in ppm, J in Hz): 6.23 (dd, 1H, $J_{trans} = 15.144$, $J_{cis} = 8.236$, H_2C═C*H*), 6.08 (dd, 1H, $J_{gem} = 1.828$, $J_{trans} = 15.144$, H*H*C═CH–), 5.63 (dd, 1H, $J_{gem} = 1.828$, $J_{cis} = 8.236$, *H*HC═CH–), 3.3 (q, 2H, NH–C*H*$_2$–CH$_2$–), 1.52 (m, 2H, NH–CH$_2$–C*H*$_2$–(CH$_2$)$_9$–CH$_3$), 1.24 (m, 18H, NH–CH$_2$–CH$_2$–(*CH*$_2$)$_9$–CH$_3$), 0.86 (t, 3H, NH–CH$_2$–CH$_2$–(CH$_2$)$_9$–*CH*$_3$).

2.3. Synthesis of copolymer

Copolymers were prepared at two different mole ratios of monomers (Fig. 1, Table 1) in DMF solvent at 60 °C using AIBN as a radical initiator with slight modification of the procedure described by Sato and coworkers [16]. A representative polymerization procedure (SAVal/DA(0.09), Table 1) is as follows: sodium *N*-acryloyl-L-valinate (SAVal) (3.0 g, 0.021 mol) and *N*-dodecylacrylamide (DA) (1 g, 0.0042 mol) were dissolved in 20 mL of DMF in a 100 mL three-neck round bottom flask equipped with a magnetic

Table 1
Copolymer composition, specific rotation, molecular weights, and polydispersity index (PDI) of SAVal–DA(0.09) and SAVal–DA (0.16) copolymers.

Copolymer	DA(x) in feed	$[\alpha]_D^{25}$	M_w (g/mol)	M_n (g/mol)	M_w/M_n
SAVal–DA(0.09)	0.09	−8.25°	396,400	225,822	1.76
SAVal–DA (0.16)	0.16	−9.88°	1,355,507	1,173,739	1.15

stirrer, a thermometer and, a condenser connected to a long gas delivery needle to serve as a gas escape valve. The solution was purged with dry, oxygen free nitrogen for 45 min at 333 K. AIBN (1 mol% of the total monomer concentration) dissolved in DMF was added via syringe. The resulting copolymers come out as precipitate from the solution as polymerization continued. However, the reaction was carried out for 24 h for achieving full conversion of the monomers. For complete precipitation, the mixture was poured into large excess of acetone. The polymer was purified by reprecipitation from methanol with acetone three times and, dissolved in pure water. After complete dissolution the solution was dialyzed against alkaline water (pH 9–10) for one weak using cellulose tube (12,000–14,000 g mol^{-1} molecular weight cut-off) to remove low molecular weight oligomers. Finally the purified polymer was recovered by freeze-drying.

2.4. Gel permeation chromatography

Gel permeation chromatography (GPC) was performed for determination of molecular weight and molecular weight distribution for the copolymers in their acid form in DMF, with a Spectra Physics Instruments equipped with a Shodex RI-101 refractometer detector and two 300 mm columns thermostated at 343 K (columns mixed-D PL-gel 5 μm from Polymer Laboratories). The flow rate was set at 0.8 mL min^{-1} using DMF as the mobile phase and the elution of the sample was monitored with RI (refractive index) detector. The elution times were converted to molecular weights with a calibration curve constructed from narrow polydispersity polystyrene standards (5×10^2–4×10^6 g mol^{-1}) from Polymer Laboratories. The calculation of molecular weight and polydispersity index was done by Millenium software (version 4.0).

2.5. General instrumentation

^{1}H NMR spectra were recorded on a Bruker SEM 200 instrument using TMS (trimethyl silane) as standard. In case of D_2O as a solvent acetonitrile was used as a reference. The UV–vis spectra were recorded in a Shimadzu (model 1601) spectrophotometer. The optical rotation was measured with Jasco P-1020 digital polarimeter. Melting points were determined with an Instind (Kolkata) melting point apparatus in open capillaries. Solid samples were weighed with a semi-micro-analytical balance (model: CP225D, Sartorious). The pH measurements were done with a digital pH meter Model pH 5652 (EC India Ltd., Kolkata) using a glass electrode. All the measurements were carried out at room temperature (~303 K) and in phosphate buffer (20 mM) at pH 8 unless otherwise mentioned.

2.6. Solution preparation

A stock solution containing 3 g L^{-1} polymer was prepared by dissolving the appropriate amount of polymer in 20 mM phosphate buffer (pH 8.0) containing 0.1 M NaCl. Solutions for analysis were prepared by dilution of the stock solutions using the same buffer solution and were allowed to equilibrate for at least 24 h at room temperature. For fluorescence measurements, the polymer stock solution (3 g L^{-1}) was made by using phosphate buffer either containing a known concentration of fluorescent probe or saturated with the probe. Dilutions were made using the same buffer solution containing the probe molecule. All measurements started after 24 h of sample preparation.

2.7. Surface tension measurement

The surface tension (γ) of the copolymers was measured using Du Nuoy ring detachment method with a 'Torsion Balance' surface tensiometer (Hurdson & Co., Kolkata) at ~303 K. Ethanol–HCl solution was often used for cleaning the platinum ring and it was burnt in oxidizing flame by use of a Bunsen burner. The instrument was calibrated through loading proper weight (for 600 mg the γ shows 49 mN m^{-1}) and checked by measuring the surface tension of distilled water before each experiment. A stock solution of copolymer was made in alkaline phosphate buffer solution (pH 8). Aliquot of this solution was transferred to a beaker containing known volume of same buffer solution. Magnetic stirring for 30 s followed by each addition of aliquot and allowed to stand for about 30 min at room temperature (~303 K) to achieve equilibrium before surface tension was measured. For each concentration, three measurements for γ were performed and their mean was taken as the value of the equilibrium surface tension.

2.8. Viscosity measurement

Viscosities of aqueous polymer solutions were measured by use of a glass Ubbelohde viscometer (ASTM-D-446) with a flow time of 180 s for pure water immersed in water bath maintained at 303 K. The density measurement was performed by use of portable digital density meter (Densito 30 PX, Mettler-Toledo, GmbH). All measurements were carried out at room temperature (~303 K) unless otherwise mentioned. Sample solutions were prepared following the same protocol as described above. Flow-through times of copolymer solutions at various concentrations (0.2–2.5 g L^{-1}) were determined at least five times for each concentration. Specific viscosities were determined by comparison with flow-through times of phosphate buffer of pH 8.

2.9. Steady-state fluorescence spectra

The steady-state fluorescence spectra of pyrene were measured with a SPEX Fluorolog-3 spectrofluorometer. The pyrene solutions were excited at 335 nm and the emission was recorded in the wavelength range 350–500 nm. The samples containing NPN were excited at 340 nm and emission was collected in the range 360–550 nm. The excitation and emission slit with band-pass equal to 1 nm was used for fluorescence measurements. In all experiments, background spectra, either of the buffer alone or of the buffer containing polymers were subtracted from the corresponding sample spectra. Stock solutions of pyrene and NPN were prepared by adding the compound to buffer solution and magnetically stirred for 24 h. The excess compound was removed by centrifugation followed by filtration through Millipore syringe filter (0.22 μm).

Steady-state fluorescence anisotropy (r) measurements of DPH probe were performed on a Perkin–Elmer LS-55 spectrophotometer equipped with an automated polarization accessory, which uses the L-format instrumental configuration according to the procedure described elsewhere [20]. The temperature of the samples was controlled using the water jacketed magnetically stirred cell holder in the spectrometer connected to Thermo Neslab RTE-7 circulating water bath that enables the temperature control of ±0.1 °C.

2.10. Fluorescence lifetime measurements

Fluorescence lifetimes were determined from time-resolved intensity decays by the method of time-correlated single-photon counting using a picosecond diode laser at $\lambda = 370$ nm (IBH, UK, nanoLED-07) as the light source for excitation. The decay kinetics of DPH was recorded at the emission wavelength of 460 nm. The typical response time of this excitation source was 70 ps. The decays were analyzed using IBH DAS-6 decay analysis software. For all the lifetime measurements, the fluorescence decay curves were analyzed by a fitting program provided by IBH. Goodness of fits was evaluated by the χ^2 value (0.9–1.3) criterion and visual inspection of the residuals of the fitted function to the data.

2.11. Light scattering measurements

The dynamic light scattering (DLS) measurements were carried out using a home-built light scattering spectrophotometer equipped with a 100 mW He–Ne laser source ($\lambda = 532$ nm) at one arm of a goniometer, at varying scattering angles ($\theta = 40°$, 60°, 80°, 90°, 100°, and 120°). The scattered beam was collected by a photomultiplier tube (PMT) detector, mounted on other arm of the goniometer, and fed to a 256-channel digital correlator (7132 Malvern, UK) with 50 ns initial delay time. The temperature was set at 298 K, unless changed to set other values. Prior to the measurements, each solution was cleaned by centrifuging at a speed of 5000 rpm for 15 min and then loaded into an optical quality cylindrical quartz sample cell. The sample cell was placed in a borosilicate glass cuvette containing an index matching liquid (*trans*-decalene) at 298 K for 30 min prior to measurement.

In a DLS measurement the observed normalized intensity autocorrelation functions $g^{(2)}(t)$ recorded with a multiple-tau digital correlator are related to the normalized field autocorrelation function $g^{(1)}(q, t)$ via Siegert relation.

$$g^{(2)}(q,t) = A + \beta\left|g^{(1)}(q,t)\right|^2 \quad (1)$$

where β is the spatial coherence factor for the detector. To obtain the size distribution the inverse Laplace transform (ILT) analysis for $g^{(1)}(t)$ was performed by using the CONTIN regularization algorithm, provided by Malvern, according to the equation.

$$g^{(1)}(t) = \int \tau A(\tau)\exp(-t/\tau)\mathrm{d}t \quad (2)$$

where τ is the relaxation time. The translational diffusion coefficient was obtained from the fitting of $g^{(1)}(t)$ and is defined as, $D = (\Gamma/q^2)_{q\to 0}$, where $\Gamma = 1/\tau$ is the relaxation rate and q represents magnitude of scattering wave vector, $q = (4\pi n/\lambda)\sin(\theta/2)$ (where θ is the scattering angle and 'n' is the refractive index of the solvent). The corresponding hydrodynamic radius (R_h) of the polymer aggregate was obtained using the Stokes–Einstein equation, $D = k_B T/(6\pi\eta R_h)$, where k_B is the Boltzmann constant and η is the solvent viscosity at temperature T.

2.12. Transmission electron microscopy

Transmission electron micrographs were obtained with a JEOL-JEM 2100 (Japan) electron microscope operating at an accelerating voltage of 200 kV at room temperature. A 5 μL volume of solution (0.1 and 0.5 g L^{-1}) was placed on a 400 mesh size carbon-coated copper grid, allowed to stand for 1 min. The excess liquid was blotted with filter paper, air-dried. The specimens were kept in desiccators overnight for drying before measurement.

3. Results and discussion

3.1. Molecular characterization of the copolymers

The polymeric structure of the compounds was suggested by the observation of disappearance of the C=C bond stretching frequency (1600 cm^{-1}) of the acrylamide monomers in the FT-IR spectrum. Further, the disappearance of the vinylic proton signal and broad peaks in the ^{1}H NMR spectra (see Fig. 1S of "Supporting Information") the copolymers confirmed polymerization of the monomers. Normally ^{1}H NMR spectrum is used to determine copolymer composition. But unfortunately, the broad bands in the ^{1}H NMR spectra did not allow us to extract any fruitful information regarding the copolymer composition. However, for structurally similar copolymers, Kawata et al. reported that the copolymer composition was virtually same as the composition in the monomer feed used for polymerization [16] These authors have also demonstrated that the effect of polydispersity on the copolymer composition is not significant. Therefore, in this work, the copolymer compositions of the polymers were assumed to be equal to the monomer feed composition of the polymerization reaction. Thus assuming a degree of polymerization of about 100 there are on average, 9 and 16 dodecyl groups in copolymers SAVal–DA(0.09) and SAVal–DA(0.16), respectively. Specific rotation values (Table 1) show that the polymer possesses chirality and it is not much different from the amino acid monomer.

The weight average molar mass (M_w) of the copolymers, SAVal–DA(0.09) and SAVal–DA(0.16) was determined by GPC. The chromatograms shown in Fig. 2S of "Supporting Information" exhibit two well-separated molecular weight distributions for both copolymers. In both polymers, the peak at higher elution volume was found to be sharp and weaker in intensity. However, a broad peak was observed at low elution volume range which was used for the analysis. The results of the analysis are summarized in Table 1. It can be observed that M_w of SAVal–DA(0.16) is almost four times higher than that of SAVal–DA(0.09). Also the former copolymer has relatively lower PDI suggesting narrower molecular weight distribution. It should be noted that the molar masses of both copolymers are quite high compared to the copolymer synthesized by Sato and coworkers [16].

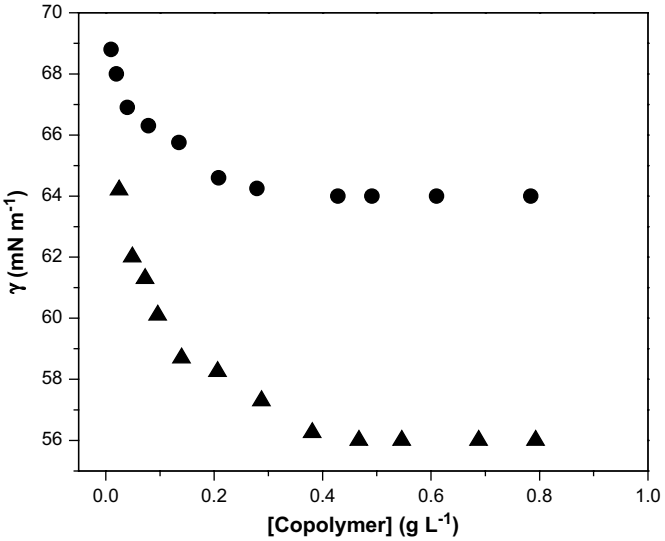

Fig. 2. Surface tension (γ) versus concentration (g L^{-1}) plots: (●) SAVal–DA(0.09) and (▲) SAVal–DA(0.16) at 303 K.

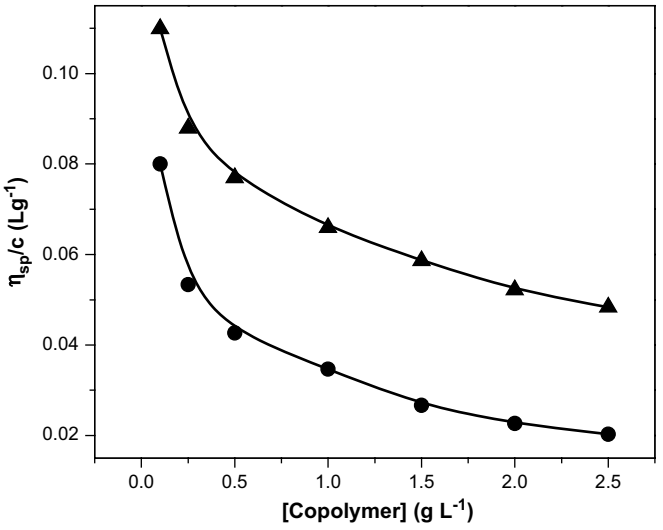

Fig. 3. Plot of reduced viscosity (η_{sp}/c) versus polymer concentration (g L^{-1}) in phosphate buffer of pH 8 at 303 K; (●) SAVal–DA(0.09), and (▲) SAVal–DA(0.16).

3.2. Surface activity of the copolymers

Fig. 2 illustrates the equilibrium surface tension (γ) for SAVal–DA(0.09), and SAVal–DA(0.16) as a function of polymer concentration in aqueous buffer solution of pH 8 at 303 K. The plots show surface tension of water gradually decreases as polymer concentration increases. It appears from the plots that SAVal–DA(0.09) with 9 mol% hydrophobic group is sufficiently hydrophilic to hinder the hydrophobic collapse of the polymer chain and packing at the air–water interface. However, as the hydrophobe content increases to 16 mol%, the packing at the surface is favored, thus causing the surface tension to decease to an equilibrium value of $\sim$56 mN m^{-1}. Small decrease of surface tension of water suggests that the amphiphilic copolymers are less surface active compared to fatty acid soaps.

3.3. Solution viscosity

To further study the solution behavior of the copolymers, viscosity experiments were performed in aqueous buffer solution of pH 8. Fig. 3 illustrates the plot of reduced viscosity as a function of copolymer concentration. The Huggins plot obtained for the copolymers was found to be non-linear in the studied concentration range, showing decrease of reduced viscosity with the increase of polymer concentration. This might be due to the formation of charged spherical aggregates. Similar results have also been reported for hydrophobically modified cationic polymers [21].

3.4. Fluorescence probe studies

To examine formation of hydrophobic domains, the fluorescence probe studies were performed using NPN as a probe molecule. Fluorescence properties of NPN are frequently used in biology [22,23] for measurements of membrane permeability induced by different biological events as well as in the characterization of the aggregates formed by synthetic surfactants [24] or amphiphilic polymers [25]. In aqueous medium, NPN exhibits a very weak fluorescence with emission maximum (λ_{max}) at 460 nm. The position of the emission maximum of NPN exhibits a blue shift in going from water to less polar solvent. While emission maximum is sensitive to polarity change the intensity rise is a function of viscosity of the medium. The NPN probe being hydrophobic in nature normally gets solubilized in the hydrophobic core of micelles, which is indicated by the large blue shift of the λ_{max} accompanied by a huge enhancement of fluorescence intensity. Thus the nature of the hydrophobic domains and the onset of hydrophobic association of aqueous polymer solutions for the copolymers can be probed by measuring the change in wavelength shift, $\Delta\lambda$ ($=\lambda_{water} - \lambda_{sample}$) and intensity ratio at different polymer concentrations relative to that in water. The representative emission spectra of NPN in presence of water as well as in 0.1 g L^{-1} copolymer solution are presented in the inset of Fig. 4(b). The plots of variation of $\Delta\lambda$ and relative fluorescence intensity (I/I_0) with polymer concentration have been depicted in Fig. 4(a) and (b), respectively. It is observed that for both copolymers the $\Delta\lambda$ and I/I_0 increased substantially as the polymer concentration is increased reaching plateau at a concentration above ca. 1.0 g L^{-1}. This suggests the incorporation of NPN in the hydrophobic domain of the aggregate. The existence of concentration-independent region in dilute solutions in both types of plots is an indication of inter-chain polymer association which might be a consequence of the hydrophobic interaction among the dodecyl chains of interacting polymer chains. The critical association concentrations (CACs) of the copolymers are 9×10^{-4} and 4.5×10^{-3} g L^{-1} for SAVal–DA(0.16) and SAVal–DA(0.09), respectively. The CAC value of SAVal–DA(0.09) is five times that of SAVal–DA(0.16). This is perhaps due to the higher hydrophobe content of the copolymer compared to SAVal–

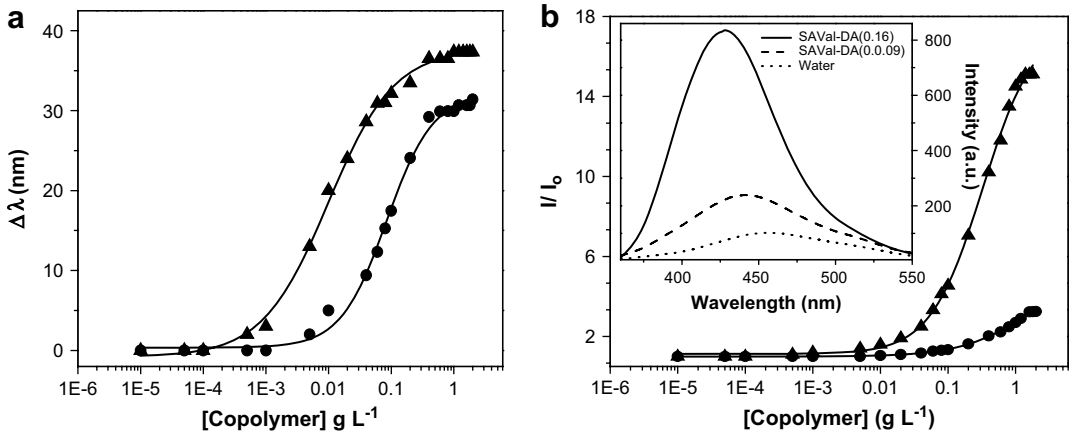

Fig. 4. Plot of (a) emission maximum shift ($\Delta\lambda = \lambda_{water} - \lambda_{sample}$), (b) relative fluorescence intensity (I/I_0) of NPN versus polymer concentration at 303 K; (●) SAVal–DA(0.09), and (▲) SAVal–DA(0.16); [Inset: NPN spectra in presence of water and 0.1 g L^{-1} copolymer solution].

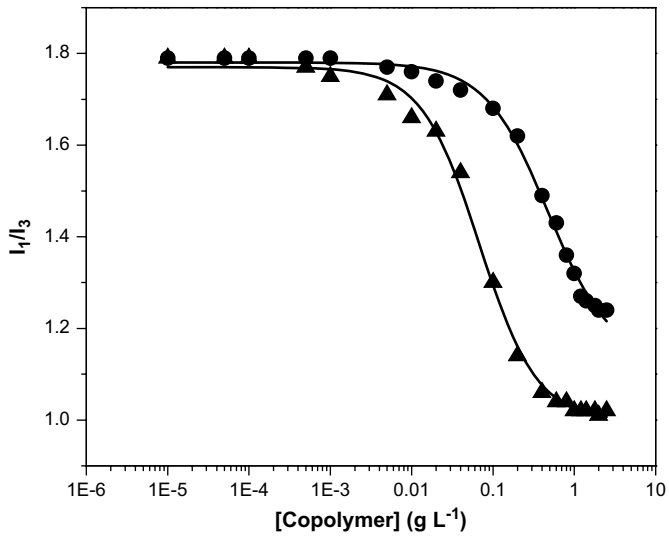

Fig. 5. Plot of intensity ratio (I_1/I_3) of pyrene versus polymer concentration: (●) SAVal–DA(0.09), and (▲) SAVal–DA(0.16) at 303 K.

DA(0.09). This is further indicated by the spectral shift values (39 nm versus 33 nm) corresponding to the plateau region of the plots in Fig. 4(a). Similarly the intensity rise is also much higher in the case of SAVal–DA(0.16). These observations clearly suggest stronger inter-chain hydrophobic interactions in the copolymer with higher hydrophobe content. As the probability of finding two-alkyl chain next to one another becomes greater hydrophobic association becomes stronger in SAVal–DA(0.16). Thus the microenvironment of NPN probe is much less polar in the aggregate formed by SAVal–DA(0.16) copolymer compared to that of SAVal–DA(0.09). Also as discussed above relatively larger I/I_0 value of NPN fluorescence in the presence of SAVal–DA(0.16) is indicative of higher viscosity of the microenvironment. However, the different behavior of the copolymers might also be partly due to molecular weight difference. The molecular weight of SAVal–DA(0.16) polymer being about 3 times higher than that of SAVal–DA(0.09) the polymer chain is more flexible and thus facilitates hydrophobic interactions and entanglement with other polymer chains.

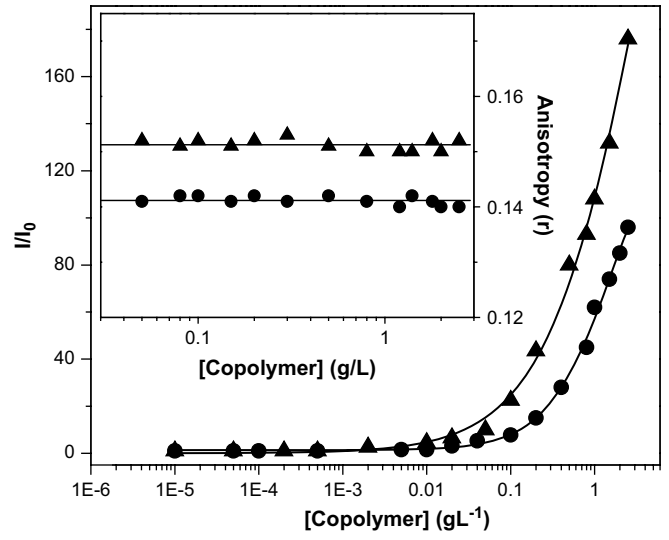

Fig. 6. Variation relative fluorescence intensity (I/I_0) of DPH probe with [copolymer] at 303 K; (●) SAVal–DA(0.09), and (▲) SAVal–DA(0.16). [Inset: Variation fluorescence anisotropy (r) of DPH probe with the concentration of (●) SAVal–DA(0.09), and (▲) SAVal–DA(0.16) at 303 K].

3.5. Micropolarity of copolymer aggregates

The micropolarity of the microdomains was estimated using pyrene as a fluorescent probe. The intensity of the vibronic bands of pyrene fluorescence spectrum strongly depends upon the polarity of the environment. Therefore, intensity ratio of the first (I_1, 372 nm) to the third (I_3, 384 nm) vibronic bands of the pyrene fluorescence spectrum is commonly used as an indicator of the apparent micropolarity [26,27]. The I_1/I_3 ratios measured in presence of different polymer concentrations are plotted in Fig. 5. The CAC values obtained from the inflection point of these plots are closely equal to those obtained from fluorescence titration using NPN probe. The value of I_1/I_3 is very low compared to water (1.82), which indicates that the microenvironment of the probe is highly non-polar. The highly non-polar microenvironment of the self-assemblies is also indicated by the large blue shift in the emission maximum ($\Delta\lambda$) of NPN spectrum. The value of I_1/I_3 is lower for SAVal–DA(0.16) compared to that of SAVal–DA(0.09), which suggests that the polarity of the microenvironment of the probe decreases with the increase of hydrophobe content.

3.6. Microviscosity of copolymer aggregates

The huge rise of fluorescence intensity in Fig. 4(b) upon incorporation of NPN probe in the copolymer aggregates of SAVal–DA(0.16) and SAVal–DA(0.09) as mentioned earlier suggests that the microenvironment of the probe is not only hydrophobic but also viscous in nature. The plots show that the intensity rise is much higher in the case of SAVal–DA(0.16) which means that the microenvironment is more rigid compared to that in the copolymer aggregates of SAVal–DA(0.09). In order to investigate the rigidity of the microenvironments of the copolymer aggregates, we have employed DPH as a fluorescent probe. The DPH molecule is a well-known membrane fluidity probe and has been used for studying many lipid bilayer membranes [28–30]. The molecule is almost insoluble in water and thus weakly fluorescent. Upon its solubilization in the hydrophobic microdomains of micelles its fluorescence intensity is enhanced. The DPH molecules preferably intercalate between the alkyl chains in the hydrophobic interior core of the micelles [31]. The steady-state fluorescence anisotropy (r) of DPH probe reflects the microviscosity (more appropriately microfluidity) of surfactant and polymer aggregates. Therefore, we have measured r of DPH in presence of the copolymers. The intensity of DPH fluorescence was observed to increase with the increase of polymer concentration. Fig. 6 depicts the plots of I/I_0 of DPH fluorescence as a function of copolymer concentration. Both plots in the figure show an inflection with concentration-independent region suggesting interpolymer aggregation and thus substantiate the results obtained from the studies with NPN probe.

Like fluorescence intensity, only the probe molecules already solubilized inside the microdomains give the r-value of DPH. The r-values of the probe measured in the presence of the copolymers (1 g L^{-1}) have been included in Table 2. The r-values ($\approx$0.15) for the copolymers are higher than that of micelles of ionic surfactants,

Table 2
Fluorescence lifetime (τ_f), pre-exponential factors (a), χ^2, fluorescence anisotropy (r) and microviscosity (η_m) of DPH probe in the aggregate of 1 g L^{-1} SAVal–DA(0.09), and SAVal–DA(0.16) in buffer solution (pH 8) at 303 K.

Copolymer	τ_f (ns)	a	χ^2	r	τ_R[a] (ns)	η_m[a] (mPa s)
SAVal–DA(0.09)	1.95	0.46	1.18	0.140	3.22	44.36
	5.27	0.53				
SAVal–DA(0.16)	2.03	0.32	1.11	0.151	6.57	87.80
	9.83	0.67				

[a] Values were calculated using longer lifetime component of DPH fluorescence.

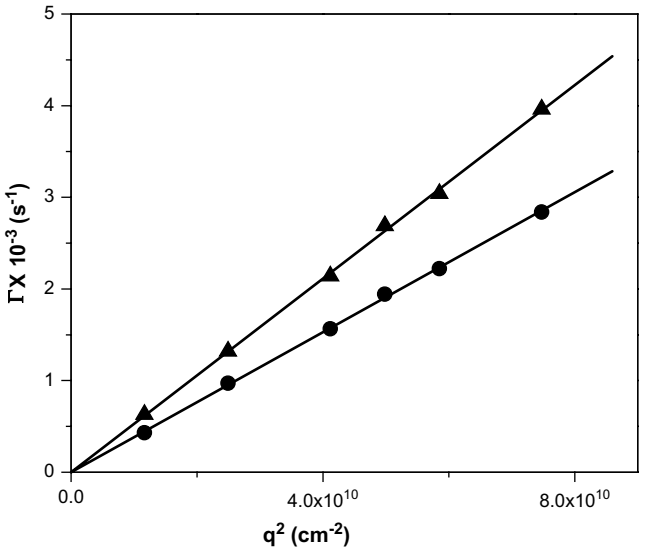

Fig. 7. Plots of relaxation rates (Γ) as a function of the square of the magnitude of the scattering vector (q^2) in 0.25 g L^{-1} polymer solution containing 0.1 M NaCl at 298 K; (●) SAVal–DA(0.09), and (▲) SAVal–DA(0.16).

such as SDS ($r = 0.054$) [20], or CTAB ($r = 0.058$) [20]. This suggests that the microenvironments of the hydrophobic domains of the copolymers are more viscous compared to surfactant micelles. The increased microviscosity might be due to lower mobility of the dodecyl chains which are covalently bound to the polymer backbone. It should be noted that *r*-value is slightly higher in the case of SAVal–DA(0.16) copolymer which means that *r*-value increases with the increase of hydrophobe content of the copolymer. However, as shown in Fig. 6 (inset), the *r*-value remains independent of concentration above CAC value of the copolymers. This might be indicative of the absence of any further aggregation or conformational change of the copolymers.

In order to estimate the microviscosity of the microdomains formed by the copolymers in aqueous solutions, we have performed time-resolved fluorescence measurements with the DPH probe. The fluorescence lifetime (τ_f) value serves as a sensitive parameter for exploring the local environment around a fluorophore [32,33], and it is sensitive to excited state interactions. The fluorescence lifetime of the DPH probe was measured in the presence of 1 g L^{-1} copolymer. In both the cases, the experimental intensity decay profile fits better to two exponential decay functions with χ^2 values in the range 1.1–1.2. The fluorescence lifetime values along with the corresponding amplitudes (a) are listed in Table 2. The existence of a large lifetime component indicates that the DPH molecules are partitioned into the viscous hydrophobic environment of the copolymer aggregates. Microviscosity (η_m) of the aggregates was calculated from the *r*- and τ_f-values of DPH using the method reported in the literature [20]. As can be observed, the microviscosity values of the hydrophobic domains are in the range 40–80 mPa s. These values are larger compared to the micelle forming DTAB, and SDS surfactants. The low mobility of the hydrophobe chains in the microdomains is due to the fact that they unlike surfactant monomers, which are in dynamic equilibrium with micelles, are covalently linked to the polymer backbone. The higher value of η_m in the case of the copolymer containing higher hydrophobe content suggests that the polymer chains are more compact compared to that in the copolymer with lower hydrophobe content. The η_m values are thus consistent with the higher hydrophobicity of the microdomains of the two types of copolymers aggregates.

3.7. Size of copolymer aggregates

The hydrodynamic diameters of the copolymer aggregates were calculated using relaxation rates (Γ) obtained from DLS measurements. The relaxation rates were first measured at various scattering angles in the range of 40–120° for a given concentration of both copolymers. Fig. 7 shows the plots of Γ as a function of the

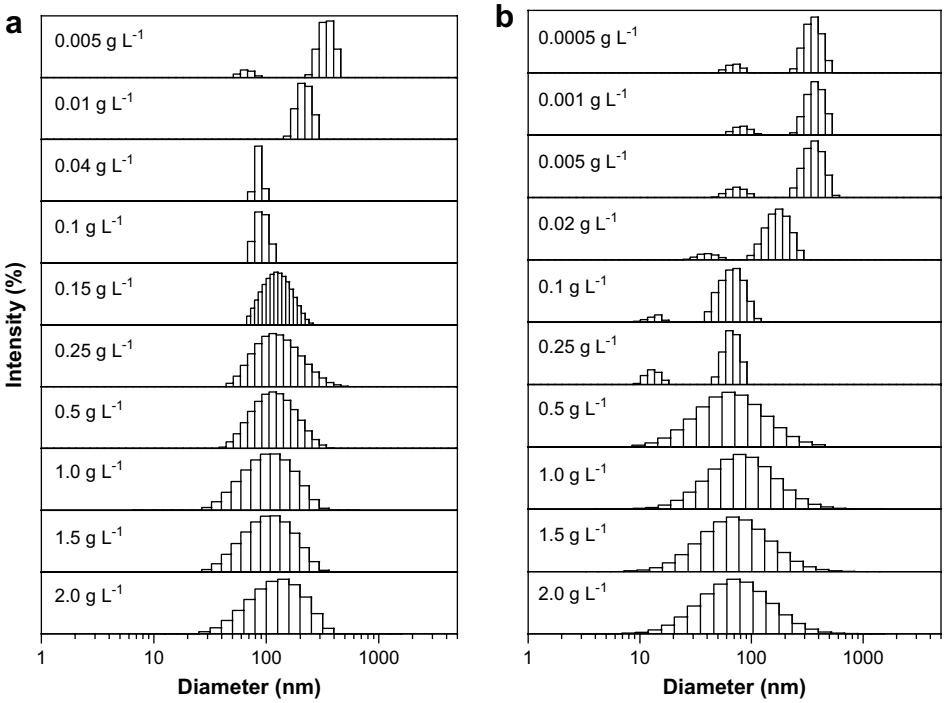

Fig. 8. The size distributions for (a) SAVal–DA(0.09), and (b) SAVal–DA(0.16) in the concentration range of 5×10^{-3}–2.0 g L^{-1}.

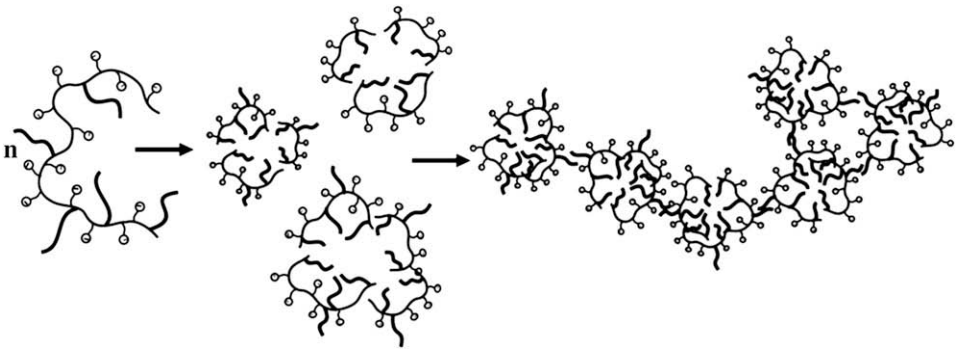

Chart 1. Conceptual representation of aggregates formed by the copolymers, SAVal–DA(0.16) and SAVal–DA(0.09) in aqueous solution.

square of the scattering vector (q). The linearity of the plots that pass through the origin clearly suggests translational diffusion of the scattering particles. The DLS measurements were performed at different concentrations of the copolymers. The size distributions thus obtained for both copolymers have been depicted in Fig. 8. It can be observed that both polymers exhibit bimodal size distributions at lower concentrations and unimodal distributions at higher concentrations. At concentrations below CAC the hydrodynamic diameter of the smaller particles is about 80 nm. On the other hand, the size of the larger particles is about 500 nm for SAVal–DA(0.16) and 200 nm for SAVal–DA(0.09) copolymer. This probably suggests that the polymer molecules have two well-separated molecular weight distributions as shown by the GPC chromatograms (see Fig. 2S of "Supporting Information"). Both shorter and longer chain polymers distribute mostly in open conformation with excess surface charge density at concentrations below the CAC value. However, with the increase of polymer concentration the average size of both types of polymer chains decreases. The size of the shorter and longer chain polymers is reduced to about 20 nm and 100 nm, respectively. In fact, at a much

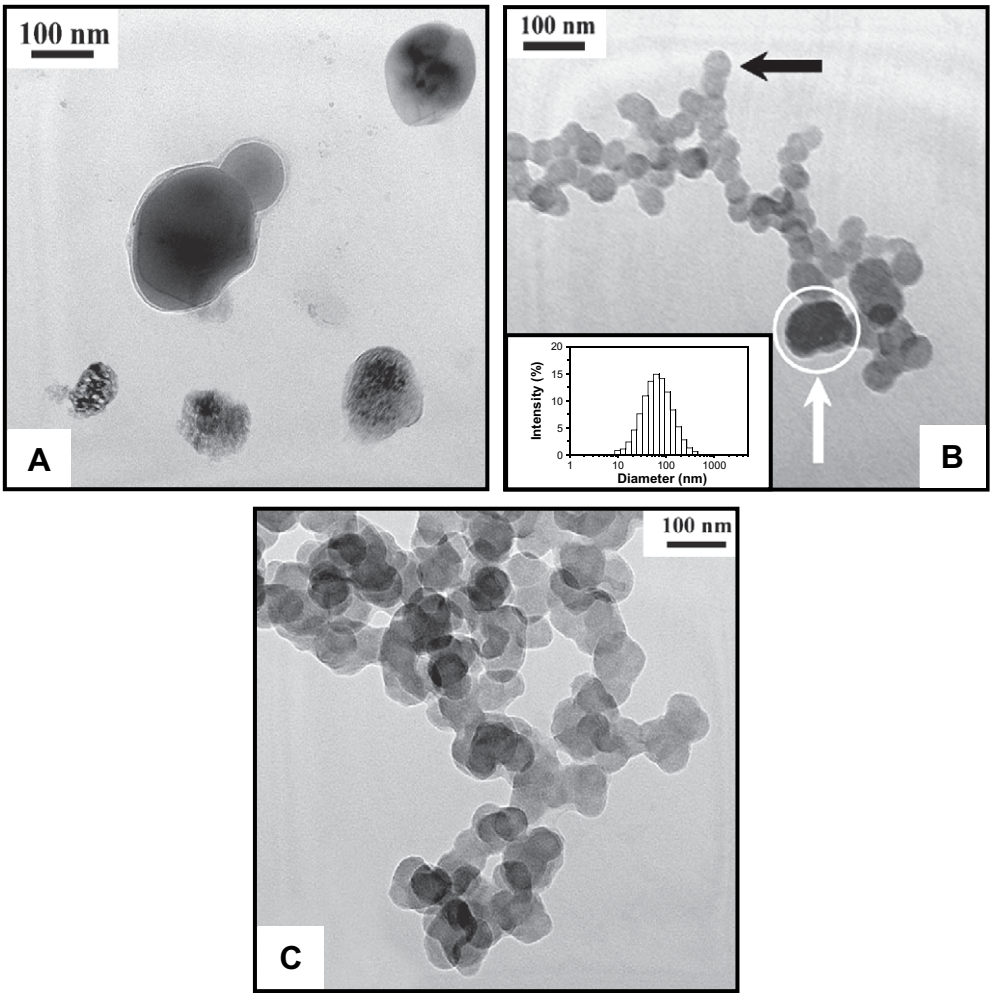

Fig. 9. TEM pictures of the copolymer solutions: (A) 0.1 g L^{-1} SAVal–DA(0.09), (B) 0.5 g L^{-1} SAVal–DA(0.16), and (C) 0.5 g L^{-1} SAVal–DA(0.09).

higher concentration above CAC the smaller particles disappear and the distributions become very broad. This can be attributed to the inter-chain aggregation of the copolymers. Thus the hydrophobic association of the copolymers is confirmed by the DLS measurements. Since the sizes of the aggregates are much higher than 5 nm, the formation of intra-chain aggregate (unimer micelles) can be eliminated. This can be assumed rather as an aggregate of shorter chain with few polymer units forming a single micellar core. However, the average diameter is around 80–100 nm corresponding to the inter-chain aggregate of several polymer units, called as multiple polymeric micelles which usually grow in numbers as well as in size with increase in polymer concentration due to the stronger hydrophobic interaction resulting in an increase of hydrodynamic diameter with broad distribution, as reported by others [16]. This is indicated by the concentration-independent fluorescence anisotropy change of DPH probe at higher polymer concentrations (inset of Fig. 6). The aggregation behavior of the copolymers can thus be presented as shown in Chart 1.

3.8. Transmission electron microscopy

To visualize the shape of the copolymer aggregates we have taken TEM pictures of the polymer solutions at two different concentrations (0.1, and 0.5 $g\,L^{-1}$). The micrographs have been depicted in Fig. 9. The micrographs at lower concentration reveal existence of isolated spherical aggregates of individual micelles in the range of 50–200 nm for SAVal–DA(0.16) (micrograph A). However, at this low concentration very few structures were detected over a large number of grid holes and owing to weak hydrophobic interaction some also appear to have some kind of irregular shape. Surprisingly, as the polymer concentration is increased from 0.1 to 0.5 $g\,L^{-1}$, the hydrophobic interaction greatly enhanced and smaller spherical particles with almost uniform sizes were observed for both the SAVal–DA(0.16), and SAVal–DA(0.09) copolymers with homogeneous inner density and a well-defined darker contour. These are found to interconnect with each other by forming branched structures. The network of interconnected micelles thus observed looks like a string of beads which might form with evaporation of the solvent, leading to an increase in density of the micelles and a corresponding decrease in their distance. However, the aggregates of SAVal–DA(0.09) (micrograph C) seem to have broader size distribution compared to those of SAVal–DA(0.16) in agreement with the corresponding PDI values (Table 1). The higher hydrophobe content of the SAVal–DA(0.16) copolymer with stronger hydrophobic interaction makes the aggregate more compact thus reducing the aggregate size. Furthermore, it can be argued that the aggregates observed from the TEM picture are obviously not formed through hydrophobic interaction of a single polymer chain (unimer micelles), which usually appears at ~5–7 nm, rather different polymer chains forming a single micellar core (shown by black arrow). Closer observation suggests that even some of the micelles in the range of 100 nm diameter appear for SAVal–DA(0.16) (micrograph B) are group of several individual micelles (as shown by white arrow). These apparently reveal stronger hydrophobic interaction of dangling chain, which forces the individual micelles to fuse in bigger compound micelles. This is also substantiated by the higher value of hydrodynamic diameter with comparatively broad size distribution obtained by DLS measurement (shown in the inset).

4. Conclusions

The results described above suggest that the copolymer chains of SAVal–DA(0.09) and SAVal–DA(0.16) undergo intermolecular association with the increase of concentration to form large multipolymer unicore micelles. Unlike the results reported by others for structurally similar copolymers we have not observed very small aggregates having hydrodynamic diameters in the range 3–10 nm corresponding to the formation of unimer micelles. This is perhaps due to the large size of the polymers compared to those already reported in the literature. The micropolarity and microviscosity of the hydrophobic domains of the micellar aggregates are much lower and higher, respectively, than that of surfactant micelles. Thus if an encapsulated drug requires increased solubility but longer retention profile, the hydrophobic domain of the SAVal–DA(0.09), and SAVal–DA(0.16) copolymers may be more useful than the micellar aggregate of synthetic surfactants. Moreover, the surface charge of the spherical aggregates can prevent fusion thus increasing their stability in aqueous environment. The study of drug solubilization and release properties of these copolymers is underway and will be reported in a future paper.

Acknowledgments

The authors gratefully acknowledge BRNS, DAE (Grant No. 2006/37/17/BRNS/235) and MHRD for financial support of this work. P.D. thanks CSIR (09/081(0519)/2005-EMR-I) for a research fellowship. The authors are thankful to Dr. N. Sarkar, Department of Chemistry, IIT, Kharagpur, and Dr. N. Chattopadhyay, Jadavpur University, Kolkata for their assistance with the DLS, and fluorescence lifetime measurements, respectively.

Appendix. Supplementary data

Supplementary data associated with this article can be found in the online version, at doi:10.1016/j.polymer.2008.12.049.

References

[1] (a) Kohn J. In: Chasin M, Langer R, editors. Biodegradable polymers as drug delivery systems. New York: Dekker.; 1990;
(b) Anderson JM, Spilizewski KL, Hiltner A. In: Williams DF, editor. Biocompatibility of tissue analogs, vol. 1. Boca Raton, Florida: CRC Press; 1985.
[2] Lehn J. Angew Chem Int Ed Engl 1988;27:89–112.
[3] Lehn J. Angew Chem Int Ed Engl 1990;29:1304–19.
[4] Sanda F, Endo T. Macromol Chem Phys 1999;200:2651–61.
[5] Blaschke G. Angew Chem Int Ed Engl 1980;19:13–23.
[6] Angiolini L, Caretti D, Carlini C, Salatelli E. Macromol Chem Phys 1995;196:2737–50.
[7] Methenitis C, Morcellet J, Pneumatikakis G, Morcellet M. Macromolecules 1994;27:1455–60.
[8] Barbucci R, Casolaro M, Magnani A. J Controlled Release 1991;17:79–88.
[9] Casolaro M, Barbucci R. Int J Artif Organs 1991;14:732–8.
[10] Casolaro M. React Polym 1994;23:71–83.
[11] Chung DJ, Ito Y, Imanishi Y. J Appl Polym Sci 1994;51:2027–33.
[12] Casolaro M. Macromolecules 1995;28:2351–8.
[13] Casolaro M, Barbucci R. Polym Adv Technol 1996;7:831–8.
[14] Bentolila A, Vlodavsky I, Ishai-Michaeli R, Kovalchuk O, Haloun C, Domb AJ. J Med Chem 2000;43:2591–600.
[15] Dutta P, Patra T, Dey J. Emerging trends in polymer science and technology. National Symposium, Kharagpur, India; 2006. p. 105–10.
[16] Kawata T, Hashidzume A, Sato T. Macromolecules 2007;40:1174–80.
[17] (a) Alexandridis P. Curr Opin Colloid Interface Sci 1996;1:490–501;
(b) Nishiyama N, Kataoka K. Adv Polym Sci 2006;193:67–101;
(c) Lukyanov AN, Torchilin VP. Adv Drug Delivery Rev 2004;56:1273–89.
[18] Iwakura Y, Toda F, Suzuki H. J Org Chem 1967;32:440–3.
[19] Morishima Y, Kobayashi T, Nozakura S. Polym J (Tokyo) 1989;21:267–74.
[20] Roy S, Mohanty A, Dey J. Chem Phys Lett 2005;414:23–7.
[21] Nichifor M, Lopes S, Bastos M, Lopes A. J Phys Chem B 2004;108:16463–72.
[22] Overath P, Träuble H. Biochemistry 1973;12:2625–34.
[23] Träuble H, Overath P. Biochim Biophys Acta 1973;307:491-–512.
[24] (a) Mohanty A, Patra T, Dey J. J Phys Chem B 2007;111:7155–9;
(b) Khatua D, Gupta A, Dey J. J Colloid Interface Sci 2006;298:451–6;
(c) Roy S, Khatua D, Dey J. J Colloid Interface Sci 2005;292:255–64;
(d) Mohanty A, Dey J. Langmuir 2004;20:8452–9;
(e) Roy S, Dey J. J Colloid Interface Sci 2005;290:526–32.
[25] (a) Kujawa P, Tanaka F, Winnik FM. Macromolecules 2006;39:3048–55;
(b) Nayak RR, Roy S, Dey J. Colloid Polym Sci 2006;285:219–24;
(c) Mohanty A, Patra T, Dey J. J Phys Chem B 2007;111:7155–9;
(d) Mohanty A, Dey J. Langmuir 2007;23:1033–40.

[26] Nakajima AJ. Mol Spectrosc 1976;61:467–9.
[27] Kalyanasundaram K, Thomas JK. J Am Chem Soc 1977;99:2039–44.
[28] (a) Shinitzky M, Barenholz Y. J Biol Chem 1974;249:2652–7;
(b) Shinitzky M, Dianoux AC, Gitler C, Weber G. Biochemistry 1971;10: 2106–13.
[29] Shinitzky M. Physical methods on biological membranes and their model systems. New York: Plenum Publishing Corp.; 1984. p. 237.
[30] Shinitzky M, Yuli I. Chem Phys Lipids 1982;30:261–82.
[31] Repáková J, Eapková P, Holopainen JM, Vattulainen I. J Phys Chem B 2004;108:13438–48.
[32] Prendergast FG. Curr Opin Struct Biol 1991;1:1054–9.
[33] Chattopadhyay A, Mukherjee S, Raghuraman H. J Phys Chem B 2002;106:13002–9.